Use of Low-Temperature Thermal Alkylation to Eliminate Ink Migration in Microcontact Printed Patterns

Susan L. Brandow,*[a] Terence L. Schull,[a] Brett D. Martin,[a] Daniel C. Guerin,[b] and Walter J. Dressick*[a]

Abstract: We demonstrate aqueous hydrogel-based microcontact printing of amine ligands into solvent-templated nanocavities of chloromethylphenyl-based siloxane or thin polymer films. Migration of pyridine ligands within films following printing, which can compromise pattern fidelity, is eliminated by heat treatment of the substrate. Gentle heating (e.g., 50 °C, 5 min) leads to the efficient alkylation of mobile pyridine adsorbate by the C–Cl bonds of the film, covalently tethering the adsorbate to the surface as a pyridinium salt. Subsequent binding of a Pd-based colloid to surface pyridinium (and remaining strongly bound and immobile pyridine ligand) sites permits selective electroless metal deposition and fabrication of patterned metal films.

Keywords: alkylation · hydrogel · imprinting · metallization · microcontact printing

Introduction

Microcontact printing (μCP) is a process for pattern replication in which an elastomeric stamp bearing a pattern of surface relief is brought into contact with a substrate surface to selectively transfer ink from the stamp to the surface.[1–3] The deposited ink replicates the relief pattern of the stamp on the surface and spatially controls the subsequent deposition of any additional species, such as polymers,[4–6] inorganic materials,[7] biomaterials,[8–13] or metals.[14] In this manner, μCP has proven a useful technique for various applications, including the fabrication of displays,[15] sensors,[14] memory elements,[16] and thin-film transistor circuitry.[17, 18]

A critical aspect for the successful use of μCP in such applications is the maintenance of pattern fidelity during printing. Migration of the ink within the stamp prior to printing[9, 19] or on the substrate surface during or after printing[20, 21] can alter the critical dimensions and edge acuities of the printed high-resolution features, compromising the fidelity of the pattern transfer from the stamp to the substrate surface. Surface migration of the ink can be minimized, but not totally eliminated, through careful control of process parameters, such as the level of ink present in the stamp[22–24] and printing contact pressure,[25] or through chemical modification of the stamp.[26, 27] The use of higher-molecular-weight inks,[9, 10, 19, 28–30] which exhibit smaller surface-diffusion coefficients, can also limit surface migration.

The elimination of ink migration often requires reaction with functional groups on the substrate surface to covalently tether the ink to the substrate during printing.[11–13, 16, 31] Unfortunately, this increases the complexity and cost of the process because additional concerns such as ink reactivity and the stability or activation of the substrate surface and stability of its reactive functional groups must also now be considered. Consequently, there is a clear need to identify new covalent strategies to prevent ink migration that minimize or eliminate such concerns. In this manuscript, we present one such approach, based on ink alkylation by surface chloromethylphenyl (CMP) functional groups, as a means to control migration without the need to preactivate surface functional groups for reaction with the ink.

[a] Dr. S. L. Brandow, Dr. W. J. Dressick, Dr. T. L. Schull, Dr. B. D. Martin
Center for Bio/Molecular Science & Engineering (Code 6950)
Naval Research Laboratory, 4555 Overlook Avenue, S.W.
Washington, DC 20375-5348 (USA)
Fax: (+1) 202-767-9594
E-mail: slb@cbmse.nrl.navy.mil, wjd@cbmse.nrl.navy.mil

[b] Dr. D. C. Guerin
Gas & Surface Dynamics Branch (Code 6174)
Naval Research Laboratory, 4555 Overlook Avenue, S.W.
Washington, DC 20375-5348 (USA)

Results and Discussion

Our approach is based on the use of aqueous hydrogels as μCP stamps to selectively transfer ligand inks into hydrophobic nanocavities formed on a substrate surface.[32, 33] The nanocavities are templated by aromatic solvent intercalation during the deposition of aromatic-polymer or organosiloxane thin films, such as those possessing the CMP group, onto the substrate.[34–36] Physisorption of ligands into the nanocavities

  0947-6539/02/0823-5363 $ 20.00+.50/0

from aqueous solution or the aqueous environment of the hydrogel stamp is thermodynamically driven by favorable interactions between hydrophobic portions of the ligand and the aromatic nanocavity walls. For amine-ligand inks such as pyridine, which are capable of forming strong $\pi-\pi$ interactions with the aromatic groups comprising the nanocavity walls, physisorption readily occurs, and the hydrophilic N-ligating site retains its access to the aqueous solution. Subsequent reaction of these amine N sites with a Pd^{II} colloidal dispersion[37–39] covalently binds Pd^{II} nanoparticles, which function as catalysts for the subsequent deposition of electroless (EL) metal, to the ligand.

Figure 1 summarizes our observations and approach concerning fabrication of patterned metal features on a substrate surface by using hydrogel-based μCP of a ligand adsorbate.

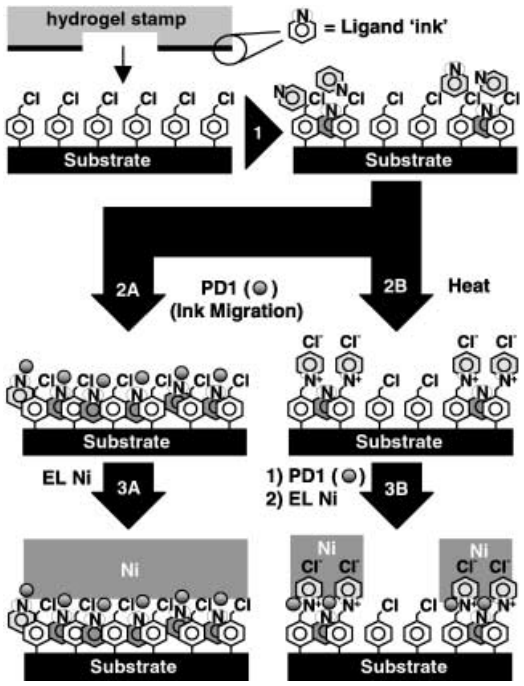

Figure 1. Hydrogel μCP patterning scheme. Printing is illustrated by using aqueous pyridine as the ligand ink, followed by the deposition of electroless Ni. Note the presence of weakly and strongly adsorbed populations of pyridine, designated by light gray and dark gray pyridine species, respectively, in panel 2. Path A shows the nonselective metallization results obtained in the absence of substrate heating due to ink migration induced by salts in the PD1 catalyst dispersion. Path B shows selective metallization of a pyridine-patterned surface due to elimination of ligand-surface migration by thermal alkylation of the pyridine adsorbate prior to catalysis and metallization.

Our initial approach involved direct stamping of pyridine or an alkylamine ligand, such as a Starburst® PAMAM Generation 2 dendrimer (SG2),[40] into the nanocavities of a poly(chloromethylstyrene) thin film coating a native-oxide Si substrate (step 1). Previous experiments[32] with SG2 had shown that little or no ink migration occurred when the patterned dendrimer was subsequently treated for 2 h with a 15 mM aqueous solution of the fluorescent dye, tetramethylrhodamine-5-(and-6)-isothiocyanate (TRITC), at pH ~ 9.

However, when we recently attempted to extend our approach to include EL metal deposition onto the pyridine or dendrimer ink pattern, behavior as shown in path A of Figure 1 was observed. In particular, treatment of the patterned surface with PD1,[38] a colloidal Pd^{II} EL metallization catalyst, provided a uniformly hydrophilic surface in the region contacted by the catalyst dispersion, consistent with transfer of the ligand adsorbate to areas of the surface not originally touched by the stamp (step 2A). In contrast, selective wetting of only those regions bearing adsorbed ink with water was observed prior to contact with the PD1 catalyst. Subsequent immersion of the catalyzed surface in an EL Ni bath deposited Ni over the entire region brought into contact with the catalyst, destroying the original stamped pattern (step 3A). Careful observation of the substrate during metal deposition revealed a differential metallization rate, with metal deposition occurring more rapidly on the areas corresponding to the original ink pattern. Various other Pd^{II}-binding ligands, including phenylalanine, sodium triphenylphosphine monophosphonate,[41] poly(allylamine), poly(2-vinylpyridine), and Starburst® PAMAM dendrimers (Generations 0 and 1), were also screened as adsorbates (see Experimental Section). In all cases, ink migration was confirmed by metallization. These observations suggest that, in contrast to previous work involving ligand-solution treatment of lithographically patterned substrates,[34–36] a substantial portion of the μCP ink was adsorbed through weaker van der Waals or hydrogen-bonding interactions.

Surface migration of the ink can occur if these weak interactions are disrupted by alterations in the structure of the surface-solution double layer induced by changes in the solution pH or ionic strength occurring during treatment with the PD1 catalyst. Treatment of the physisorbed SG2 ligand with an aqueous pH 5 morpholinoethane sulfonate buffer solution containing 0.11M NaCl (i.e., a PD1 "blank", see Experimental Section), followed by treatment with fluorescent TRITC dye, supports this hypothesis. The binding of dye in regions of the surface not originally contacted with SG2 confirms ligand migration, a behavior similar to that noted elsewhere concerning protein surface diffusion.[20]

Elimination of surface migration of printed ligand inks requires either removal of the weakly bound ligand population or conversion to a more stable linkage through chemical reaction with the surface prior to subsequent attachment of other materials, such as the Pd^{II}-catalyst nanoparticles of PD1. Extensive rinsing and/or ultrasonication of μCP samples was either ineffective in arresting ink migration or compromised the printed pattern. Alternatively, we decided to explore methods of covalently linking the printed ink to the surface-bound CMP group. In fact, surface-bound pyridinium species are known to form during the reflux of solutions of pyridine derivatives with CMP siloxane films;[42, 43] this suggests that a modified approach might be employed here to immobilize weakly bound ligands.

Consequently, we adapted this approach to function in our system by heating pyridine-impregnated CMP siloxane films prepared by our droplet-screening (see Experimental Section) or hydrogel μCP methods to initiate alkylation of the physisorbed ligand populations by the C–Cl groups of the film. Figure 2 shows an X-ray photoelectron spectroscopy (XPS) result for the N(1s) energy region after heating a

0947-6539/02/0823-5364 $ 20.00+.50/0 *Chem. Eur. J.* **2002**, *8*, No. 23

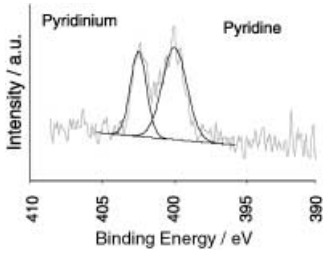

Figure 2. XPS N(1s) spectrum of a heated pyridine-impregnated CMP siloxane film. Process sequence: 1) pyridine (aq, 0.1M, 5 min); 2) Heat (50 °C, 5 min).

pyridine-impregnated CMP siloxane film for 5 min at 50 °C. Separate peaks are observed at binding energies of ~400 and ~402.5 eV. The ~400 eV peak is also observed (as the sole peak) prior to the heat treatment and is characteristic of the pyridyl N group.[34, 44] The peak at ~402.5 eV has been previously assigned to a surface-bound pyridinium N species;[42, 43] this confirms the occurrence of thermal alkylation of physisorbed pyridine in our films.[45] Alkylation efficiency, determined as the ratio of the pyridinium XPS N(1s) peak to the total XPS N(1s) signal, is ~45–50%. Increases in the heating time do not further increase the degree of alkylation; this indicates that the reaction is essentially complete within 5 min. Such a rapid reaction is not completely unexpected, given the high local concentrations and proximities of adsorbed pyridine species and C–Cl bonds in the CMP siloxane films.[46]

Alkylation also occurs at temperatures as low as ~35 °C, although the efficiency is reduced (i.e., $\lesssim$40%). At higher temperatures, alkylation efficiency increases somewhat and appears to reach a limiting value of ~60–65% for samples heated above ~65 °C. Increased variability of the total N(1s) signal relative to the Si(2p) signal from the substrate is also observed, especially for samples baked at higher temperatures. These behaviors, taken together, suggest that competitive evaporation of more weakly adsorbed pyridine ligands (b.p. ~115 °C) may play a role in limiting the observed alkylation efficiency.

The simplest model consistent with all of our experimental observations is summarized in panel 2 of Figure 1. In this model, two populations of adsorbed ink are created on the substrate surface during μCP.[20] One population comprises ligand that is strongly physisorbed inside the film nanocavities and is essentially immobile. In the second population, the ligand is weakly adsorbed through van der Waals interactions between hydrophobic portions of the ligand and the CMP groups, and/or hydrogen-bond interactions between amines of the weakly and strongly adsorbed species. Alkylation efficiency would approach a limiting value in this case if only one of the ligand adsorbate populations is capable of readily reacting with the C–Cl bonds of the CMP groups. For the pyridine population physisorbed inside the CMP nanocavities, adsorption is strong,[34–36] and molecular models suggest that the pyridine N ligand will experience difficulty in accessing the C–Cl bond due to constraints imposed by the nanocavity on its translational motion and ability to reorient itself for reaction. Consequently, alkylation is likely to involve reaction of the more mobile, weakly adsorbed pyridine ligand population with the CMP groups. Under these conditions, the alkylation efficiency represents a direct measure of the relative amount of weakly adsorbed pyridine in the film, in the absence of any evaporative losses. In fact, the limiting efficiencies of ~60–65% obtained here correspond closely to values obtained elsewhere for mobile protein-adsorbate populations on surfaces measured by alternate methods.[20] Unfortunately, our data currently preclude a more detailed analysis of the relative contributions due to multiple adsorbate populations and evaporative effects.

Regardless of the nature of the mechanism, however, substrate heating provides an effective means to eliminate ink migration in our system. Treatment of the baked substrates with PD1 catalyst, followed by EL Ni metallization, selectively deposits Ni only in those areas originally brought into contact with the ligand ink. No metallization is observed adjacent to the ligand deposition sites, in contrast to the nonselective metallization behavior previously exhibited for substrates not subjected to the baking step (vide supra). Figure 3 illustrates one example of a high-resolution metal pattern prepared by hydrogel μCP, baking, and selective metallization according to the method shown in path B of Figure 1. Metallization efficiency in this case is enhanced relative to that observed for unheated substrates due to the presence of cationic pyridinium surface species, which electrostatically bind additional negatively charged nanoparticles that comprise the PD1 catalyst, supplementing the direct covalent-binding mode associated with the pyridine sites.[34–36]

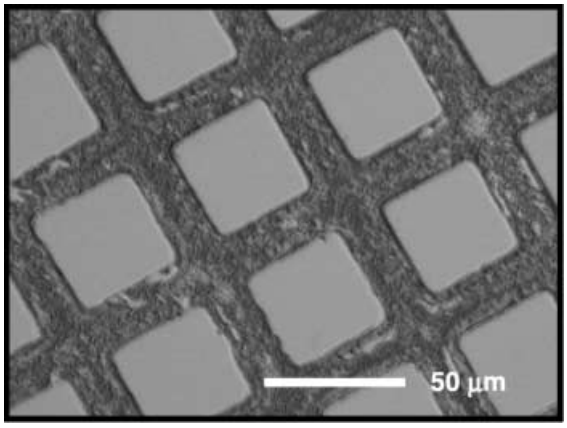

Figure 3. Optical micrograph of a Ni metal pattern formed by hydrogel-based μCP. Ni is deposited in the squares (light regions) produced by μCP by using a patterned hydrogel stamp charged with aqueous pyridine. Extraneous metallization observed in the intervening channels (dark regions) reflects imperfections in the hydrogel stamp transferred from the master during casting. Process sequence: 1) Patterned μCP (0.2M pyridine (aq), 120 s, 1.5 g, CMP siloxane film); 2) Heat (50 °C, 5 min); 3) PD1 catalyst (30 min); 4) Water rinse; 5) EL Ni (10 min).

There are several points worth noting concerning Figure 3. First, visual inspection of the patterns indicates that deposition of the Ni proceeds with good homogeneity and selectivity in the square regions comprising the ligand surface pattern defined by μCP. Pattern-transfer fidelity, as measured by the widths and center-to-center separations of the printed Ni features is also good. For example, the nominally 35.0 μm wide squares from the hydrogel stamp provide 35.1 ± 0.7 μm

wide Ni squares after metallization. Pattern placement, as measured by center-to-center separations of squares in adjacent rows, is 50.6 ± 0.8 μm compared with the nominal value of 50.0 μm from the stamp. The overall feature-edge acuity for the pattern, as measured by the standard deviation of the average feature width (i.e., ± 0.7 μm), is $\pm 2\%$. For certain individual Ni squares, however, values as large as $\pm 7\%$ are observed. Careful inspection in these cases reveals that the increase in edge roughness is associated with spurious deposition of Ni in the channel regions in contact with the feature edge, rather than any significant distortion of the printed ligand pattern during μCP. Traces of Ni deposited in these areas separating the Ni squares reflect defects in the hydrogel stamp introduced during casting. Consequently, improvements in the hydrogel stamp quality and μCP protocols are expected to provide improved feature edge acuity control in this regard.

Conclusion

The method described here offers several advantages in comparison with standard procedures involving covalent reaction of an ink with a surface functional group to prevent ink migration.[11–13, 16, 31] In particular, there is no need to preactivate the substrate surface through the formation of chemically activated species, such as carboxylic acid active esters,[12, 13] and maintain sufficient chemical reactivity of these species prior to and during μCP. The CMP groups comprising the substrate surface remain inert prior to and during the μCP process. The latent reactivity of the surface C–Cl bonds is activated only upon heating, efficiently alkylating the pyridine adsorbate at low temperatures after short reaction times. In addition, the method is substrate generic; various substrates, including inert materials such as diamond[47] or poly(tetrafluoroethylene),[48] are readily coated with adherent CMP siloxane or polychloromethylstyrene thin films by using standard microlithography film fabrication techniques.[34, 36, 49, 50] Consequently, the process represents a simple and cost-effective approach, compatible for use with commercial manufacturing track-lines, for the fabrication of patterned metal films by using an aqueous-based hydrogel μCP technique.

Experimental Section

All materials were A.C.S. Reagent Grade or better from Aldrich Chemical Co. and were used as received, except where noted. Deionized water (18 MΩ) and N_2 gas from liquid nitrogen boil-off were used where applicable for experiments. Native oxide p-type ⟨100⟩ Si wafers were obtained from Wafernet, Inc. and cleaned by using standard techniques.[37] Polychloromethylstyrene (Aldrich; 3- and 4-isomers (60:40); $M_w \sim 55\,000$ g mol^{-1}; $M_n \sim 100\,000$ g mol^{-1} (by GPC/malls); Lot #HW-01025EW) was dissolved in toluene (1% wt. solution) and spin-coated onto Si wafers that had been vapor primed with hexamethyldisilazane to form polymer films according to the literature procedure.[51] Freshly distilled 4-chloromethylphenyltrichlorosilane (142–144 °C/15 mm Hg; Gelest) was used in toluene for the preparation of CMP siloxane films as described previously.[52]

The PD1 EL catalyst was prepared according to the literature procedure.[38] A NIPOSIT® Ni468B EL bath (pH ~ 7, Shipley Co.) was prepared according to the manufacturer's instructions and diluted to 10% strength with water prior to use in order to slow metal deposition and prevent delamination of the Ni layer. Briefly, the substrate to be Ni plated was contacted with PD1 (~30 min), gently rinsed in water, and immersed in the EL Ni bath (~10 min, 25 °C). After removal from the EL Ni bath, the substrate was rinsed with water and dried in a filtered stream of N_2 gas. Additional information for the metallization process is presented in detail elsewhere.[49, 50]

Ink migration screening experiments were performed prior to μCP as follows: Three droplets (~20 μL) of an aqueous ligand (~0.1 M) or polymer ligand (1% wt.) solution were placed in a triangle pattern on the CMP siloxane or polychloromethylstyrene films. The ligands used and their solution pHs, adjusted by using tetraethylammonium hydroxide or HCl, included pyridine (pH 7.5), phenylalanine (pH 9.5), sodium triphenylphosphine monophosphonate (pH 9.5),[41] and Starburst® PAMAM dendrimers (Generations 0, 1, and 2; all pH 9.5). Polyallylamine HCl ($M_w \sim 8000$–$11\,000$ g mol^{-1}, Aldrich, Lot TG13713MG, pH 9.5) and poly-2-vinylpyridine ($M_w \sim 40\,000$ g mol^{-1}, Scientific Polymer Products Inc., Lot 09, pH 3.7) were used as polymer ligand inks. After a 5–10 min contact time, the droplets were carefully removed by using a micropipet, and the substrate was rinsed with water.[53] Sufficient PD1 catalyst was placed on the substrate to completely cover the area previously occupied by the droplets, and the metallization process was completed as described in the previous paragraph. In one case, a blank PD1 catalyst prepared without Pd^{II} and containing only morpholinoethane sulfonate buffer (9 mM, pH 5) in aqueous NaCl (0.11 M) was used. For this experiment, the treated surface was visualized by covalently tagging the deposited Starburst® PAMAM Generation 2 ligand dendrimer with TRITC (Molecular Probes Inc., Eugene, OR) fluorescent dye by using the literature method.[32] Control experiments indicated that TRITC did not bind the CMP siloxane film in the absence of ligand.

The thermal alkylation experiments were performed with aqueous pyridine (0.1 M, pH 7.5) ink and CMP siloxane films by following a modified ink-migration screening protocol. Specifically, following removal of the ink droplets and the water rinse, the substrates were baked on a programmable vacuum hotplate (Wentworth Labs Model TC-100). Various combinations of bake temperatures (35–100 °C) and bake times (5–20 min) were investigated. After the samples had cooled to room temperature, they were cleaved in half. One portion of each sample was brought into contact with the PD1 catalyst, immersed in the EL Ni bath, and visually examined to determine the extent and quality of the Ni plate.

The second portion of each sample was analyzed by XPS with a Fisons (220ixL) spectrometer equipped with an $Al_{K\alpha}$ source, quartz monochromator, concentric hemispherical analyzer operated in the fixed-analyzer transmission mode, and multichannel detector. Spectra were acquired at a takeoff angle of 45°, and the operating pressure was $\leq 10^{-8}$ Torr. Because samples for XPS analysis were prepared on conductive Si substrates, charge compensation was not required. Minimal acquisition times were used to limit X-ray damage to the CMP siloxane. All spectra were referenced to the $Si(2p_{3/2})$ substrate peak. The degree of alkylation was defined by the ratio, $N_{402}/(N_{402} + N_{400})$, in which N_{402} and N_{400} are the areas of the N(1s) peaks due to alkylated pyridine N at ~402.5 eV[42] and unreacted pyridine N at ~400 eV,[34, 44] respectively. Uncertainties for peak-area measurements and the calculation of the degree of alkylation were typically ~10% and ~15–20%, respectively.

The preparation and use of the hydrogel stamps is described in detail elsewhere.[32, 33] Briefly, a Cu TEM grid comprising orthogonal 15 μm-diameter Cu wires separated from parallel wires by a distance of ~35 μm to form a square template was used to cast the hydrogel stamp. The stamp was equilibrated (~2 h) with an aqueous ligand (~0.1–0.2 M) or polymer-ligand solution (~1% wt.) and blown dry with N_2 gas prior to use. The μCP procedure involved fixing the hydrogel stamp in a micropositioner and contacting it under its own weight (~1.5–2.0 g, 90–300 s) with the polychloromethylstyrene film or CMP-siloxane surface to complete the ink transfer. After allowing the stamped surface to air dry (~5 min), it was brought into contact with an aqueous TRITC dye solution for fluorescent tagging, or baked and treated with an EL metallization catalyst for metal deposition (vide supra). For metallized substrates, the Ni pattern was examined by optical microscopy. Critical dimensions and edge acuities of the Ni features were measured and compared to nominal values from the hydrogel stamp to assess pattern quality by using the previously described method.[54] Calculations of the appropriate averages and standard devia-

0947-6539/02/0823-5366 $ 20.00+.50/0 *Chem. Eur. J.* **2002**, *8*, No. 23

tions utilized ~100 measurements of feature widths from nine different square Ni features and twelve measurements of center-to-center separations of adjacent Ni squares (note Figure 3).

Acknowledgement

Financial support for this work from the Office of Naval Research under the Naval Research Laboratory Core Funding Program is gratefully acknowledged. D.C.G. thanks the National Research Council for a postdoctoral fellowship.

[1] E. Delamarche, M. Geissler, H. Wolf, B. Michel, *J. Am. Chem. Soc.* **2002**, *124*, 3834–3835.
[2] B. Michel, A. Bernard, A. Bietsch, E. Delamarche, M. Geissler, D. Juncker, H. Kind, J.-P. Renault, H. Rothuizen, H. Schmid, P. Schmidt-Winkel, R. Stutz, *IBM J. Res. Dev.* **2001**, *45*, 697–719.
[3] Y. N. Xia, G. M. Whitesides, *Ann. Rev. Mater. Sci.* **1998**, *28*, 153–184.
[4] R. M. Crooks, *ChemPhysChem* **2001**, *2*, 244–254.
[5] J. Hyun, A. Chilkoti, *Macromolecules* **2001**, *34*, 5644–5652.
[6] S. Holdcroft, *Adv. Mater.* **2001**, *13*, 1753–1765.
[7] K. Ha, Y.-J. Lee, D.-Y. Jung, J. H. Lee, K. B. Yoon, *Adv. Mater.* **2000**, *12*, 1614–1617.
[8] J. S. Hovis, S. G. Boxer, *Langmuir* **2001**, *17*, 3400–3405.
[9] M. Geissler, A. Bernard, A. Bietsch, H. Schmid, B. Michel, E. Delamarche, *J. Am. Chem. Soc.* **2000**, *122*, 6303–6304.
[10] A. Bernard, J. P. Renault, B. Michel, H. R. Bosshard, E. Delamarche, *Adv. Mater.* **2000**, *12*, 1067–1070.
[11] D. W. Branch, J. M. Corey, J. A. Weyhenmeyer, G. J. Brewer, B. C. Wheeler, *Med. Biol. Eng. Comp.* **1998**, *36*, 135–141.
[12] Z. Yang, A. M. Belu, A. Liebmann-Vinson, H. Sugg, A. Chilkoti, *Langmuir* **2000**, *16*, 7482–7492.
[13] J. Lahiri, E. Ostuni, G. M. Whitesides, *Langmuir* **1999**, *15*, 2055–2060.
[14] D. B. Wolfe, J. C. Love, K. E. Paul, M. L. Chabinyc, G. M. Whitesides, *Appl. Phys. Lett.* **2002**, *80*, 2222–2224.
[15] Z. Y. Huang, P. C. Wang, A. G. MacDiarmid, Y. N. Xia, G. Whitesides, *Langmuir* **1997**, 13, 6480–6484.
[16] Z. Zhong, B. Gates, Y. Xia, D. Qin, *Langmuir* **2000**, *16*, 10369–10375.
[17] C. R. Kagan, T. L. Breen, L. L. Kosbar, *Appl. Phys. Lett.* **2001**, *79*, 3536–3538.
[18] J. A. Rogers, A. Dodabalapur, Z. Bao, H. E. Katz, *Appl. Phys. Lett.* **1999**, *75*, 1010–1012.
[19] E. Delamarche, H. Schmid, A. Bietsch, N. B. Larsen, H. Rothuizen, B. Michel, H. Biebuyck, *J. Phys. Chem. B* **1998**, *102*, 3324–3334.
[20] L. Szyk, P. Schaaf, C. Gergeley, J. C. Voegel, B. Tinland, *Langmuir* **2001**, *17*, 6248–6253.
[21] P. E. Sheehan, L. J. Whitman, *Phys. Rev. Lett.* **2002**, *88(156104)*, 1–4.
[22] T. L. Breen, P. M. Fryer, R. W. Nunes, M. E. Rothwell, *Langmuir* **2002**, *18*, 194–197.
[23] L. Libioulle, A. Bietsch, H. Schmid, B. Michel, E. Delamarche, *Langmuir* **1999**, *15*, 300–304.
[24] Y. Xia, G. M. Whitesides, *Langmuir* **1997**, *13*, 2059–2067.
[25] C. Y. Hui, A. Jagota, Y. Y. Lin, E. J. Kramer, *Langmuir* **2002**, *18*, 1394–1407.
[26] J. Hyun, A. Chilkoti, *J. Am. Chem. Soc.* **2001**, *123*, 6943–6944.
[27] J. L. Tan, J. Tien, C. S. Chen, *Langmuir* **2002**, *18*, 519–523.
[28] H. Li, D.-J. Kang, M. G. Blamire, W. T. S. Huck, *Nano Lett.* **2002**, *2*, 347–349.
[29] R. C. van Duijvenbode, G. J. M. Koper, M. R. Böhmer, *Langmuir* **2000**, *16*, 7713–7719.
[30] M. Liebau, J. Huskens, D. N. Reinhoudt, *Adv. Funct. Mater.* **2001**, *11*, 147–150.
[31] Y. Jun, D. Le, X.-Y. Zhu, *Langmuir* **2002**, *18*, 3415–3417.
[32] B. D. Martin, S. L. Brandow, W. J. Dressick, T. L. Schull, *Langmuir* **2000**, *16*, 9944–9946.
[33] K. W. Rhee, L. M. Shirey, P. I. Isaacson, C. F. Kornegay, W. J. Dressick, M.-S. Chen, S. L. Brandow, *J. Vac. Sci. Technol. B* **2000**, *18*, 3569–3571.
[34] W. J. Dressick, M.-S. Chen, S. L. Brandow, *J. Am. Chem. Soc.* **2000**, *122*, 982–983.
[35] W. J. Dressick, M.-S. Chen, S. L. Brandow, K. W. Rhee, L. M. Shirey, F. K. Perkins, *Appl. Phys. Lett.* **2001**, *78*, 676–678.
[36] W. J. Dressick, P. F. Nealey, S. L. Brandow, *Proc. SPIE–Int. Soc. Opt. Eng.* **2001**, *4343*, 294–305.
[37] W. J. Dressick, C. S. Dulcey, J. H. Georger, Jr., G. S. Calabrese, J. M. Calvert, *J. Electrochem. Soc.* **1994**, *141*, 210–220.
[38] W. J. Dressick, L. M. Kondracki, M.-S. Chen, S. L. Brandow, E. Matijević, J. M. Calvert, *Colloids Surf. A* **1996**, *108*, 101–111.
[39] S. L. Brandow, M.-S. Chen, T. Wang, C. S. Dulcey, J. M. Calvert, J. F. Bohland, G. S. Calabrese, W. J. Dressick, *J. Electrochem. Soc.* **1997**, *144*, 3425–3434.
[40] SG2 is a dendrimer ($M_n \sim 3256\,g\,mol^{-1}$) terminated by 16 primary alkylamine groups. An aqueous solution was prepared by evaporating the commercial methanol solution (20% wt., Aldrich) to dryness under vacuum, and carefully adding the calculated amounts of deaerated water and aqueous HCl (2 M) to the dry material.
[41] T. L. Schull, J. C. Fettinger, D. A. Knight, *Inorg. Chem.* **1996**, *35*, 6717–6723.
[42] W. B. Lin, W. Lin, G. K. Wong, T. J. Marks, *J. Am. Chem. Soc.* **1996**, *118*, 8034–8042.
[43] S. B. Roscoe, S. Yitzchaik, A. K. Kakkar, T. J. Marks, Z. Xu, T. Zhang, W. Lin, G. K. Wong, *Langmuir* **1996**, *12*, 5338–5349.
[44] *Handbook of X-ray Photoelectron Spectroscopy* (Ed.: G. E. Muilenberg), Perkin-Elmer, Eden Prairie, MN **1992**.
[45] A Cl(2p) XPS signal at ~199 eV was also observed following heat treatment, consistent with the expected formation of a charge-compensating chloride ion[44] during the alkylation reaction. However, the signal exhibited a sample-to-sample variability that suggested siloxane-film damage by the X-rays during data acquisition, presumably through the formation and removal of chloride as HCl from the film. Although we attempted to limit film damage through the use of minimal data-acquisition times, quantitative analysis of the chloride signals was not possible under our experimental conditions.
[46] Previous work[34] has shown that XPS N(1s)/Cl(2p) ratios of >0.7 are observed for CMP siloxane films fully impregnated with pyridine. Given a cross-sectional area of 25 Å^2 calculated from molecular models for the CMP group, a close-packed CMP siloxane film would correspond to an effective CMP group surface density of $\sim 6.6 \times 10^{-10}$ mol CMP per cm^2. Assuming equal densities of nanocavities and CMP groups, the first approximation for a toluene-templated siloxane film yields $\sim 3.3 \times 10^{-10}$ mol CMP per cm^2 and $\sim 3.3 \times 10^{-10}$ mol nanocavities per cm^2. Using the ~0.7 fill factor from the XPS data implies a pyridine concentration of $> 2.3 \times 10^{-10}$ mol pyridine per cm^2 in the siloxane film. For the adsorption of a single monolayer of pyridine of thickness ~5 Å in the CMP siloxane film of thickness ~6 Å, these values correspond to effective molar concentrations at the surface of ~4.6 M pyridine and ~5.5 M CMP, respectively.
[47] M.-S. Chen, C. S. Dulcey, S. L. Brandow, D. N. Leonard, W. J. Dressick, J. M. Calvert, C. W. Sims, *J. Electrochem. Soc.* **2000**, *147*, 2607–2610.
[48] T. G. Vargo, J. A. Gardella, Jr., J. M. Calvert, M.-S. Chen, *Science* **1993**, *262*, 171–172.
[49] M.-S. Chen, S. L. Brandow, C. S. Dulcey, W. J. Dressick, G. N. Taylor, J. F. Bohland, J. H. Georger, Jr., E. K. Pavelchek, J. M. Calvert, *J. Electrochem. Soc.* **1999**, *146*, 1421–1430.
[50] M.-S. Chen, S. L. Brandow, W. J. Dressick, *Thin Solid Films* **2000**, *379*, 203–212.
[51] S. L. Brandow, M.-S. Chen, S. J. Fertig, L. A. Chrisey, C. S. Dulcey, W. J. Dressick, *Chem. Eur. J.* **2001**, *7*, 4495–4499.
[52] S. L. Brandow, M.-S. Chen, R. Aggarwal, C. S. Dulcey, J. M. Calvert, W. J. Dressick, *Langmuir* **1999**, *15*, 5429–5432.
[53] CMP siloxane films are sufficiently stable to withstand film hydrolysis during the experiment. UV spectroscopy of CMP siloxane films on fused-silica slides indicates only slight film loss (<5%) under our treatment conditions (pH 9.5, 10 min, 25°C). In fact, complete hydrolysis of the CMP siloxane film occurs only under more severe conditions (pH 9.5–10.0, 2–3 h, 50–60 °C).
[54] K. Koumoto, S. Seo, T. Sugiyama, W. S. Seo, W. J. Dressick, *Chem. Mater.* **1999**, *11*, 2305–2309.

Received: June 19, 2002 [F4191]